Supporting information

Highly Efficient Photocatalytic Degradation of Organic Pollutants by PANI-modified TiO_2 Composite

Yangming Lin, Danzhen Li*, Junhua Hu, Guangcan Xiao, Jinxiu Wang, Wenjuan Li, Xianzhi Fu

Research Institute of Photocatalysis, State Key Laboratory Breeding Base of Photocatalysis, Fuzhou University, Fuzhou, 350002, P. R. China

Corresponding author Tel & Fax: (+86)591-83779256, E-mail: dzli@fzu.edu.cn.

Summary: This file contains 15 pages, 12 figures.

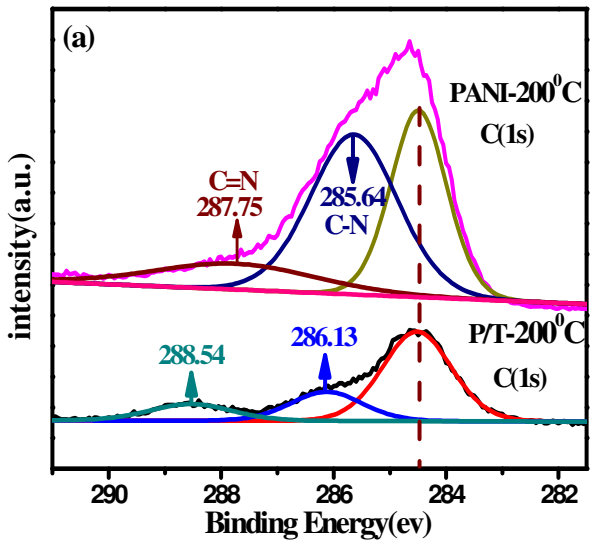
(a)
PANI-200^{0}C
C(1s)
C=N
287.75
285.64
C-N
P/T-200^{0}C
C(1s)
288.54
286.13
intensity(a.u.)
290
288
286
284
282
Binding Energy(ev)

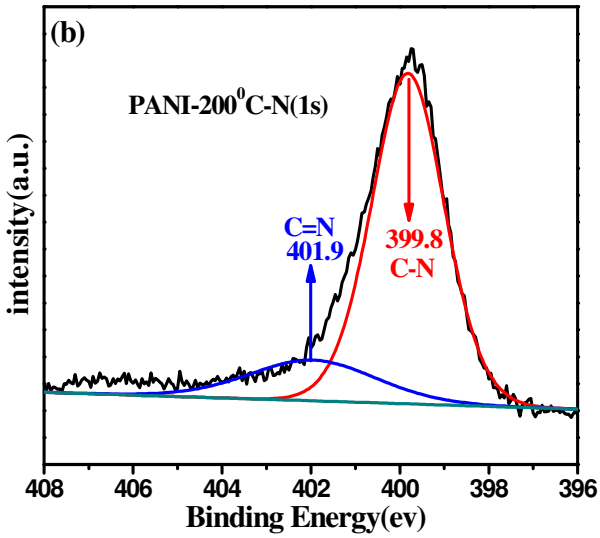
(b)
PANI-200^{0}C-N(1s)
C=N
401.9
399.8
C-N
intensity(a.u.)
408
406
404
402
400
398
396
Binding Energy(ev)

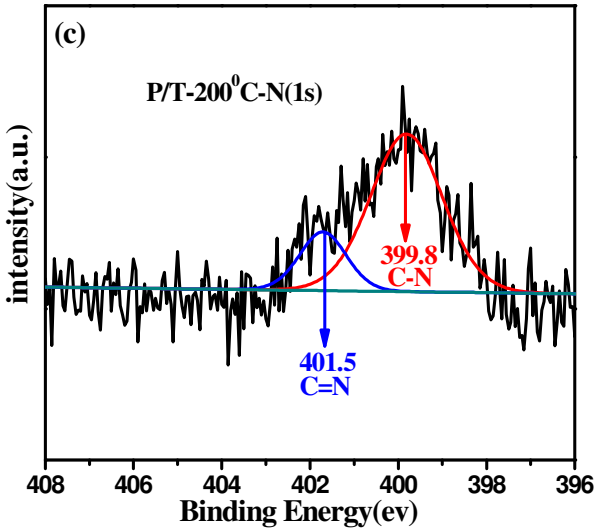
(c)
P/T-200^{0}C-N(1s)
399.8
C-N
401.5
C=N
intensity(a.u.)
408
406
404
402
400
398
396
Binding Energy(ev)

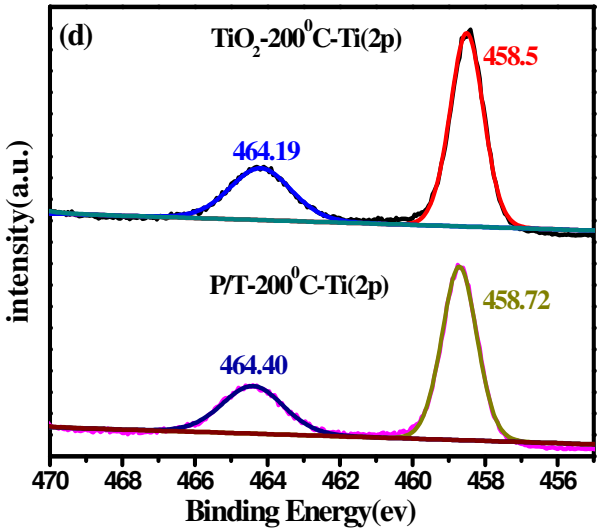
(d)
TiO$_2$-200^{0}C-Ti(2p)
458.5
464.19
P/T-200^{0}C-Ti(2p)
458.72
464.40
intensity(a.u.)
470
468
466
464
462
460
458
456
Binding Energy(ev)

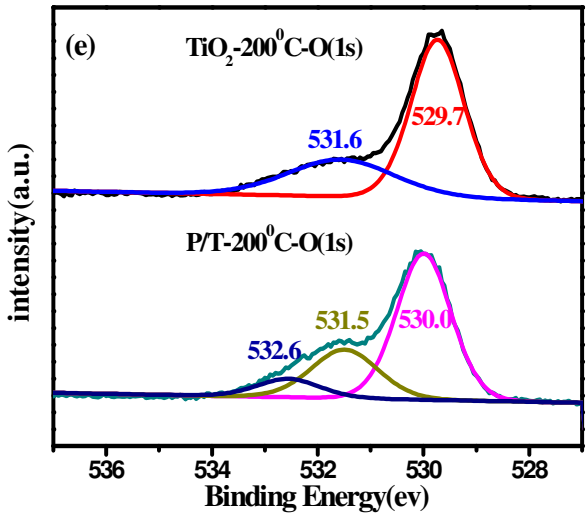

Figure S1. XPS spectra of photacatalysts: (a) C(1s) spectrum of PANI-200 °C and P/T-200 °C, (b) (c) N(1s) spectrum of PANI-200 °C and P/T-200 °C, (d) Ti(2p) spectrum of TiO_2-200 °C and P/T-200 °C , (e) O(1s) spectrum of TiO_2-200 °C and P/T-200 °C.

Note:

As shown in Figure S1 (Supporting Information), three peaks can be observed at 284.5, 285.64 and 287.75 eV for C (1s) binding energy (BE). The first at 284.5 eV is attributed to C atoms bound only to C or H atoms. The two later peaks correspond to C-N and C=N of bare PANI, respectively. Compared with PANI, the BE of C=N of P/T shifts from 287.75 to 288.54 eV, which indicates that C element links with O to form O-C=N structure. Another peak at 286.13, which originates from C=C bonds in the residual organic groups of pare TiO_2 or C-N of P/T. As mentioned in the analysis of IR of C=C bonds, there is no difference in TiO_2 and P/T and then the absence of C=C bonds interaction with other elements. However, the BE of C-N of P/T moves from 285.64 to 286.13 which reveals that other structure O-C-N maybe exist in the P/T system. Meanwhile, as shown in Figure

S1b and c, N element binding energy of pure PANI at 399.8ev and 401.9 ev can be ascribed to C-N and protonated C=N. After the PANI is used to modify TiO_2, only the C=N binding energy shifts to low BE of 401.5 ev. Comparison between Figure S1d show that the BE of Ti (2p) from 458.5, 464.19 to 458.72 and 464.4 ev, respectively. There results illustrate that the structure of O-C=N-Ti and O-C-N generate in the P/T nanocomposite. Namely, it might be related to the combination of TiO_2 nanocrystalline and PANI, which produced stronger binding force due to the interaction between TiO_2 nanoparticles and the lone pair electrons of N atom in the polymer backbone. More, three peaks at 530.0, 531.5 and 532.6 ev for P/T are classified as lattic oxygen, hydroxyl oxygen and adsorption oxygen. Compared with XRD and the differences of O (1s) spectra of P/T and TiO_2, implying O element of O-C=N-Ti and O-C-N are very likely assigned to adsorption oxygen and not lattic oxygen. In conclusion, according to the results of FTIR and XPS, there are likely to contain intensive interaction structures such as O-C=N-Ti and O-C-N in the P/T system. The further study of the detail interaction between PANI and TiO_2 is now in progress.

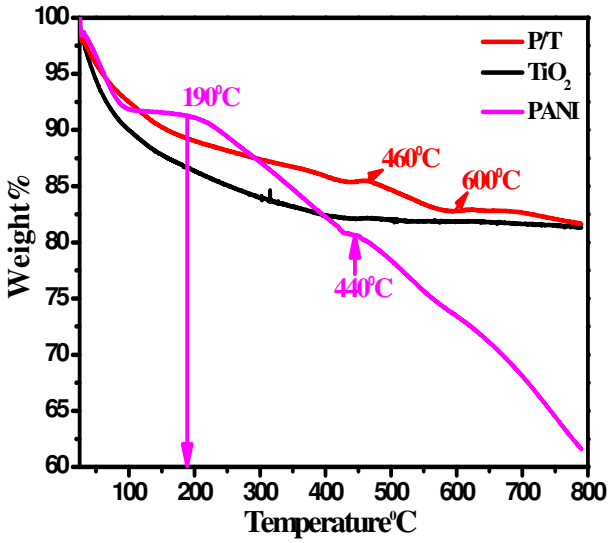

Figure S2. TG curves of PANI, TiO_2 and P/T nanocomposites.

Note:

As shown in Figure S2, it can be observed that the losses of weight of PANI occurr around three temperature periods, range from 100 °C, 190 °C and around 440 °C. The first two weight losses are mainly attributed to residual water，the elimination of impurities, and some oligomers. Another decrease of mass occurr around 440 °C is due to the degradation of polymer main chain. Similarly，there are two regions of loss of weight in the TG curve of P/T. The former from 25 °C to 460 °C results from desorption of the crystal water，the elimination of impurities, and degradation of some oligomers. The latter ranging from 460 °C to 600 °C is ascribed to degradation of polymer main chain and the phase transformation of TiO_2 from anatase to rutile.

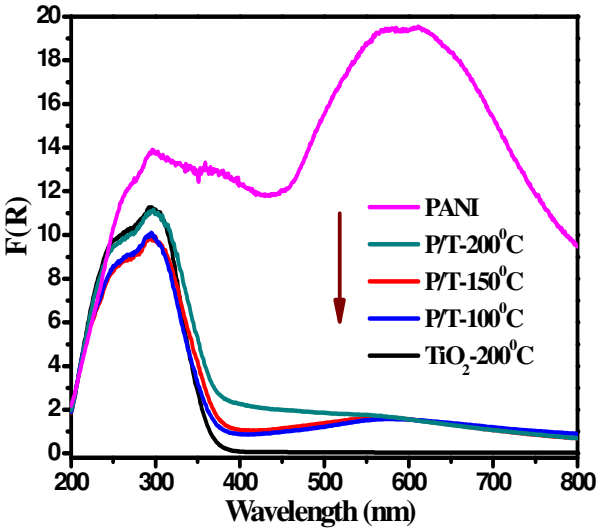

Figure S3. Optical band gap energy (Eg) of P/T, TiO_2 and PANI nanocomposites.

Note:

As displayed in Figure S3, It is also interesting to observe that the P/T nanocomposites possess much better visible light absorption intensity (400-800nm) than bare TiO_2. Thus, the presence of PANI affects significantly the visible light absorption (a red shift to higher wavelength) for the P/T nanocomposites.

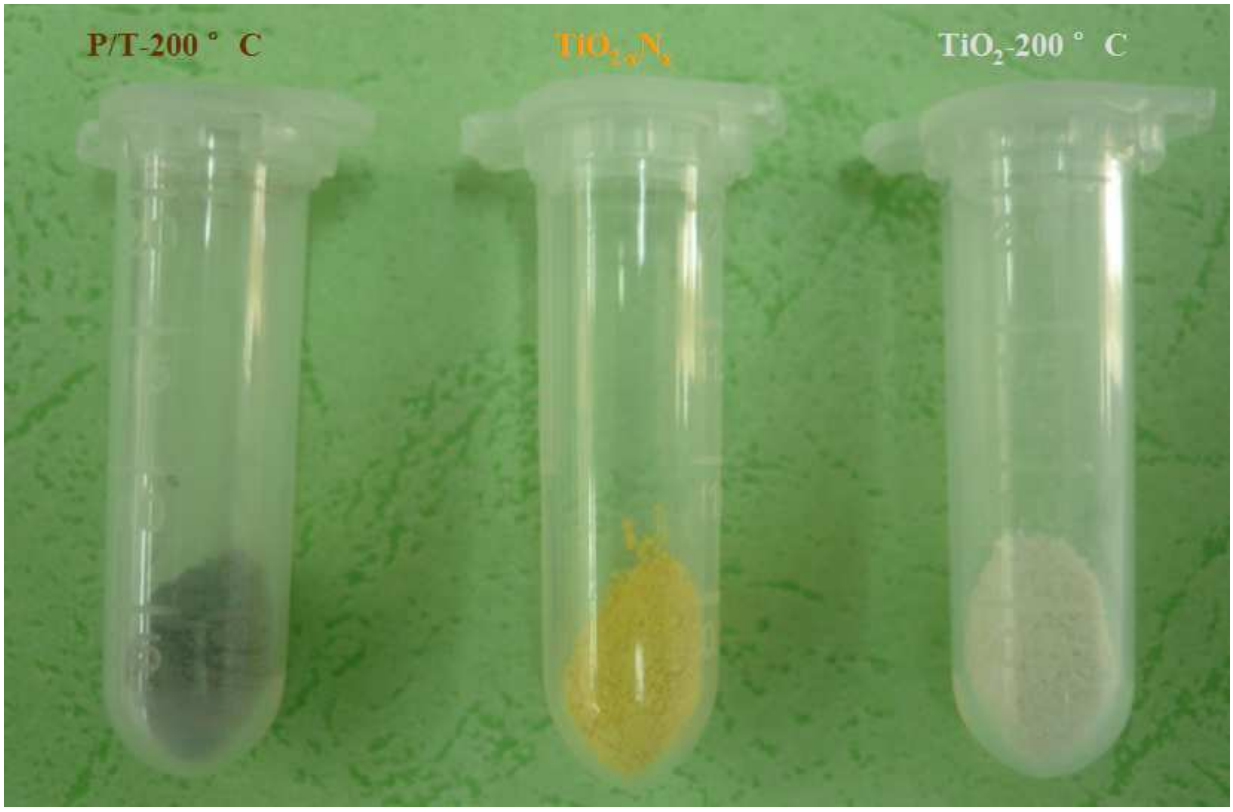

Figure S4.The images of the as-prepared photocatalysts; from left to right is P/T-200 °C, $TiO_{2-x}N_x$, TiO_2-200 °C nanocomposites, respectively.

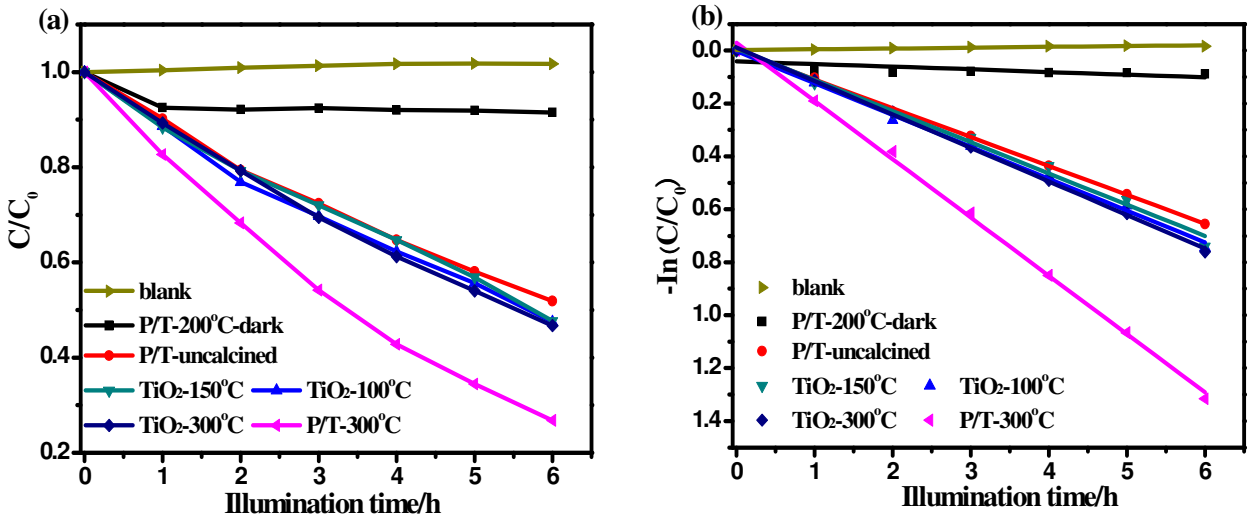

Figure S5. Liquid-phase photocatalytic degradation (a) and Kinetic linear simulation curves (b) of methylene orange (MO) over photocatalysts under visible light irradiation (420 nm <λ< 800 nm).

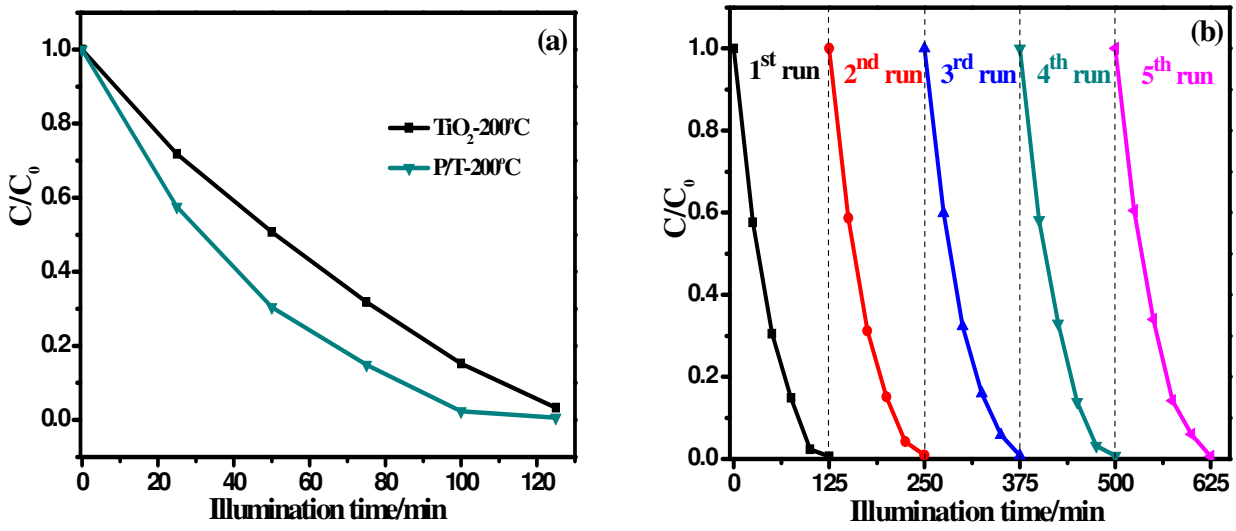

Figure S6. (a) The photodegradation of MO (20ppm) over P/T-200 °C and TiO_2-200 °C nanocomposites under UV light (λ=254nm) and (b) photodegradation stability of MO (20ppm) over P/T-200 °C nanocomposites under UV light (λ=254nm).

Note:

Besides the above mentioned visible light photoactivity, the degradation of MO (20ppm) over P/T-200 °C under UV light is slightly better than that of TiO2-200 °C is shown in Figure S6a.To further investigate its photodegradation stability, analogous the process of P/T-200 °C under UV light (254nm) is shown in Figure S6b. Undoubtedly, in this case, the P/T-200 °C also exhibits excellent photocatalytic stability.

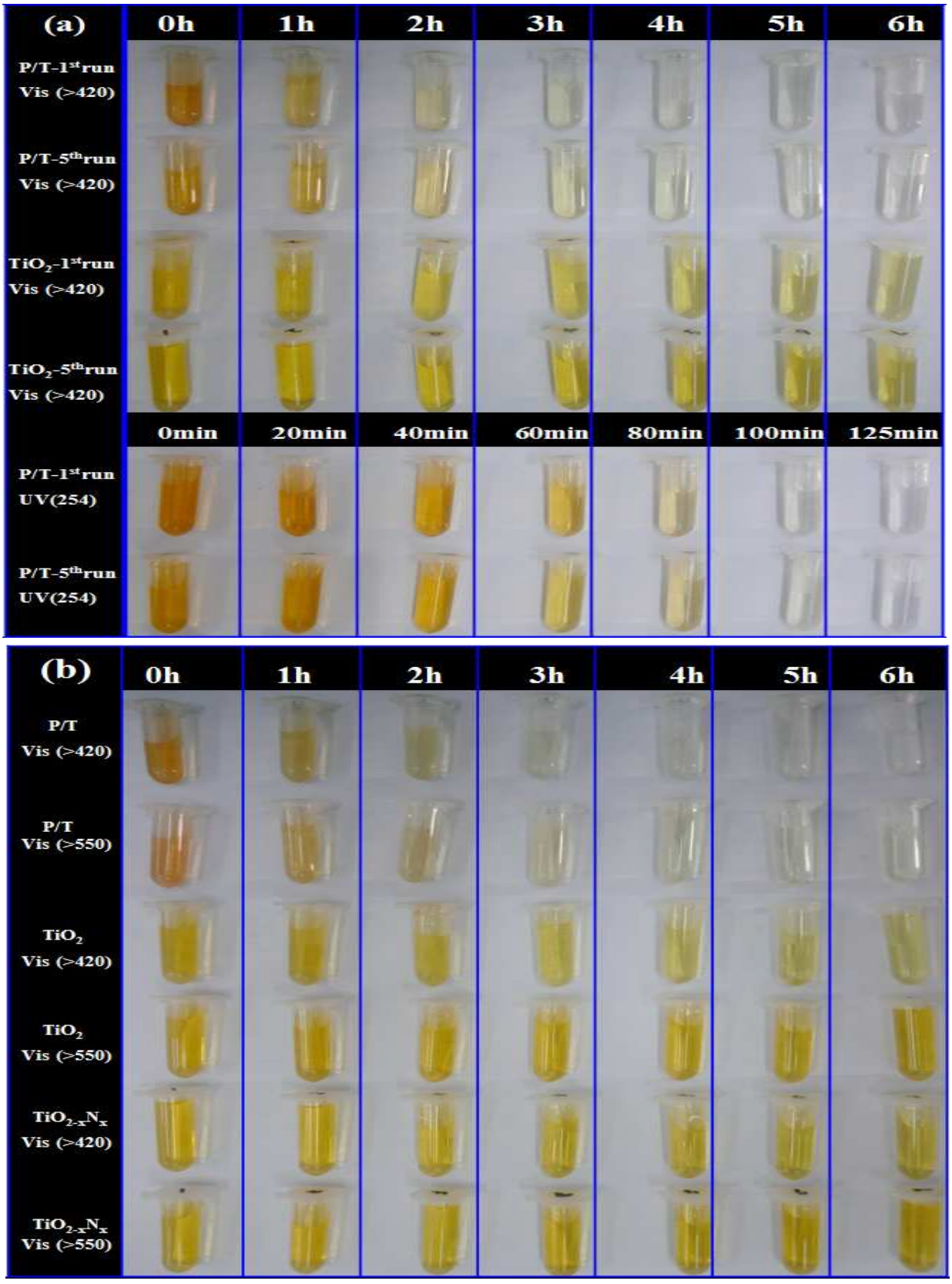

Figure S7. (a) The optical photos of Recycled photodegradation of MO under the irradation of UV and visible light over P/T-200 °C, TiO_2-200 °C nanocomposites, respectively (b) The optical photos of the degradation of MO over P/T-200 °C, TiO_2-200 °C, $TiO_{2-x}N_x$ under the visible light with

different wavelengths.

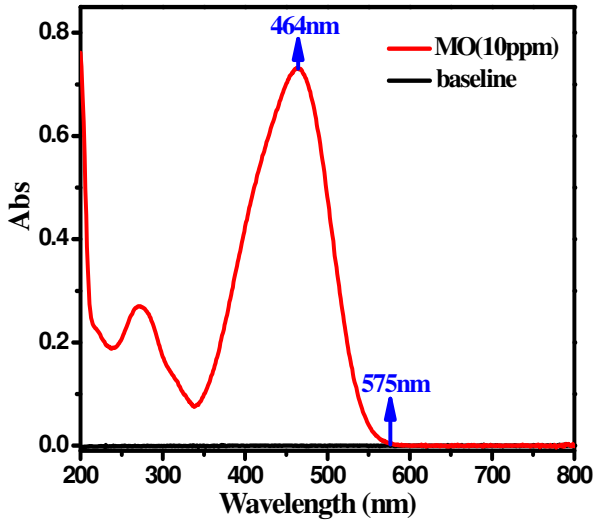

Figure S8. Absorption spectra of the MO (10ppm).

Note:

Figure S8 illustrates the maximum absorption peak of MO is at λ=464nm and the absorption spectrum of visible light up to 575nm, slightly wider than filter light wavelength 550m, these suggestion that weak activity of $TiO_{2-x}N_x$ toward the degradation of MO at 550 nm <λ< 800nm may be due to adsorption.

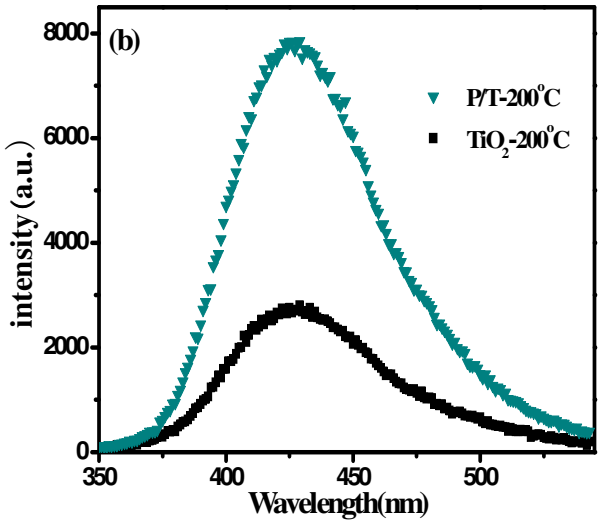

Figure S9. •OH-trapping PL spectra of P/T-200 °C and TiO_2-200 °C under visible light (420 nm < λ < 800 nm) for 6 h.

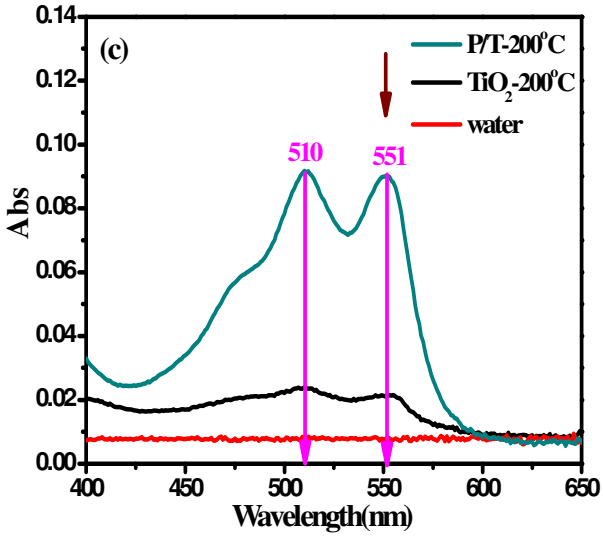

Figure S10. Detection of H_2O_2 in P/T-200 °C and TiO_2-200 °C water dispersions (photocatalyst 80mg / water 80mL) by addition of DPD and POD to the dispersions after 6 h of irradiation under visible light (420 nm < λ < 800 nm).

Note:

H_2O_2 as another important intermediate species in the photocatalysis process can occur mainly from reactions of superoxide anion radical. Compared to TiO_2 with faint peaks, TiO_2 is modified by PANI possesses more obvious absorption peaks at 510 and 551 nm when DPD and POD are added in the system. Therefore, it not only verified the existence of $O_2^{\bullet -}$ species again, but also provided another inevitable source for •OH radicals.

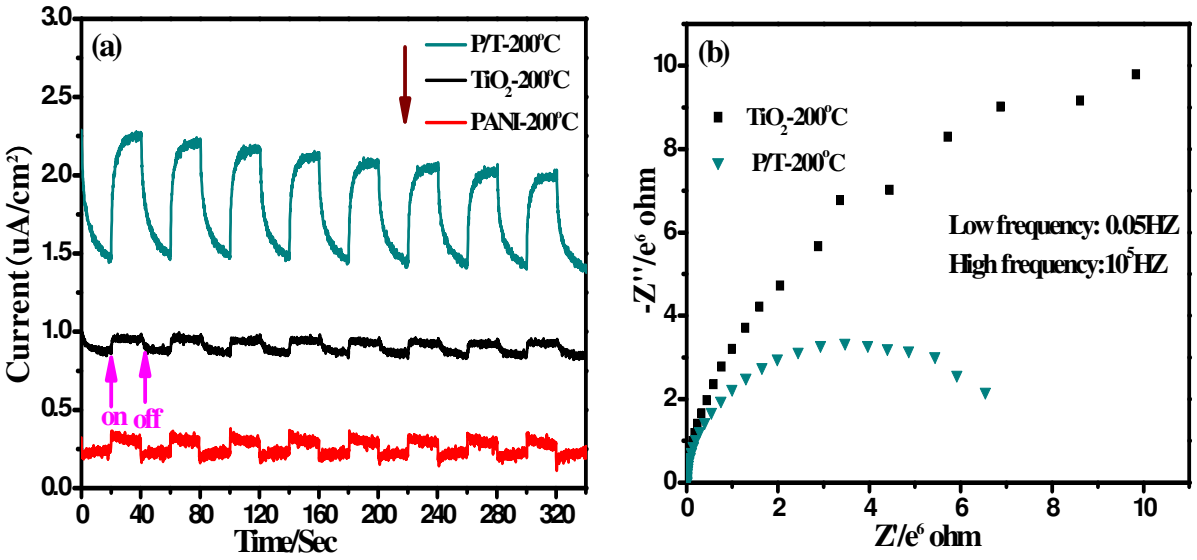

Figure S11. (a) Photocurrent spectra of P/T-200 °C, TiO_2-200 °C and pristine PANI-200 °C under the irradiation of visible light (420 nm < λ < 800 nm) (b) EIS Nynquist plots of P/T -200 °C and TiO_2-200 °C with an applied bias potential of 1.0 V under visible light (420 nm < λ < 800 nm).

Note:

As displayed in Figure S11a, when visible light source is turned on or off, the instantaneous photocurrent of pristine PANI and bare TiO_2 are in a small degree. The photocurrent of PANI results from its high mobility of charge carriers under the irradiation of visible light. That of TiO_2 is derived form carbon self-doping and visible photosensitive groups on the surface of TiO_2 can excite to genenrate the electron/hole pairs under visible light, which is also corresponding to the weak photodegradation of MO, but much smaller than after P/T. As shown in Figure S11b, it is so clearly that the radius of the arc on the EIS Nynquist plot of P/T-200 °C is smaller than that of the TiO_2-200 °C, which reflects that P/T-200 °C possesses the faster interfacial charge transfer. The results of photoelectrochemical tests are well correspond to that of photocatalytic experiments.

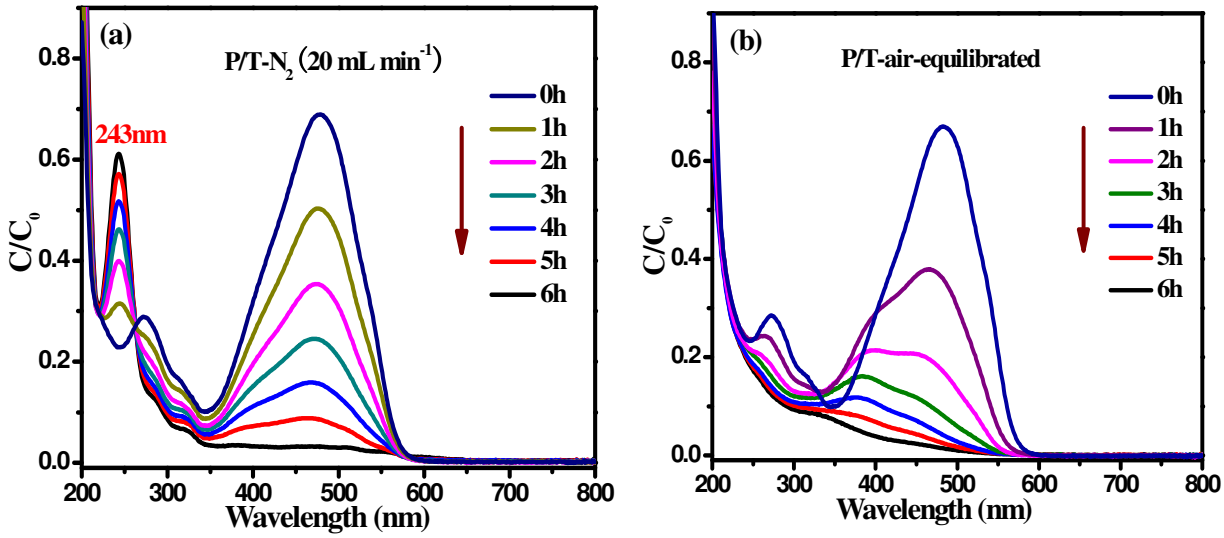

Figure S12. (a) Absorption spectra changes of the MO solution under N_2 (20 mL min^{-1}) and (b) air-equilibrated conditions in the presence of P/T-200 °C after visible light irradiation (420 nm <λ< 800 nm).

Note:

Dissolved O_2 as an efficient electron scavenger to produce a variety of active oxygen species significantly promotes the degradation process. In order to further evaluate the role of dissolved O_2 in the reaction, N_2 is bubbled through the suspension at the rate of 20mL min^{-1} to ensure that the reaction is operated without O_2. As displayed in Figure S12a, the absorption spectra are significantly changed and a new peak appears in 243nm, which is attributed to a reduction product, hydrazine. This indicats that photoreduction of MO is well catalyzed by P/T possibly through electron and hole transfer, but the hydrazine does not continue to be degradated without O_2. Namely, in the absence of O_2, MO molecules are not completely degradated and the degradation process is actually a reduced phenomenon in the P/T system. In the air-equilibrated conditions shown in Figure S12b, both of the intensities of the two main absorption peaks are decreased. Therefore, the electrons or the active species generated by electrons play an important role in the photocatalytic reaction.